Reliability analysis using a multi-metamodel complement-basis approach

Teixeira, Rui; Martinez-Pastor, Beatriz; Nogal, Maria; O'Connor, Alan

DOI
10.1016/j.ress.2020.107248

Publication date
2021

Document Version
Final published version

Published in
Reliability Engineering and System Safety

Reliability Engineering and System Safety 205 (2021) 107248

Contents lists available at ScienceDirect

Reliability Engineering and System Safety

journal homepage: www.elsevier.com/locate/ress

Reliability analysis using a multi-metamodel complement-basis approach

Rui Teixeira[a,*], Beatriz Martinez-Pastor[a], Maria Nogal[b], Alan O'Connor[c]

[a] School of Civil Engineering University College Dublin, Ireland
[b] Department of Materials, Mechanics, Management and Design, Technical University Delft, The Netherlands
[c] Department of Civil, Structural & Environmental Engineering, Trinity College, Ireland

ARTICLE INFO

Keywords:
reliability analysis
adaptive metamodeling
response surface method
polynomial chaos expansion
Kriging
complement-basis
multiple metamodel selection

ABSTRACT

The present work discusses an innovative approach to metamodeling in reliability that uses a field-transversal rationale. Adaptive metamodeling in reliability is characterized by its large spectra of models and techniques with different assumptions. As a result, the reliability engineer is frequently faced with the highly challenging task of selecting an appropriate model or technique with limited *a priori* knowledge about the performance function that defines the problem of reliability.

To tackle this challenge, a complement-basis is proposed for adaptive metamodeling. It consists in using a batch of multiple metamodels or techniques that, accordingly to an activation criterion, are selected to solve the reliability analysis. This activation is set to depend on the model synergy with the problem in-hand. In the present work the leave-one-out loss is applied as evaluator of compatibility, and results show that the absolute loss successfully performs as an activator.

A metamodel-independent learning approach and stopping criterion are implemented to study the proposed approach in five representative examples. Results show that the complement-basis allows to increase the efficiency of the reliability analysis through the selection of adequate metamodels, which is indicative of the untapped potential that further transversal research may add to metamodeling in reliability analysis.

1. Introduction

In recent years research in adaptive metamodeling for reliability analysis has increased. A metamodel surrogates the limit state function that defines the problem of reliability and, because in reliability the limit state function needs to be evaluated multiple times, it significantly reduces the effort that is required to complete the reliability assessment. When an accurate surrogate of the true performance function is set, reliability analysis becomes virtually effortless. Hence, metamodeling is an effective bypass technique to solve problems that are computationally challenging in reliability engineering, such as, reliability-based design optimization [1–4] or time-variant reliability analysis [5–7].

In the context of metamodeling for reliability, adaptive approaches have gained particular prominence due to their superior performance. Adaptive metamodeling involves the construction of measures of improvement (usually using an unsupervised learning technique) that yield accurate cost-effective surrogates. In the past different methodologies have been introduced to perform reliability analysis with the minimum number of performance function evaluations that guarantees accurate estimations of the probability of failure (P_f). As a result, one of the characteristics of the current state-of-art in the field is the existence of a plurality of metamodels and approaches to solve the same problem, where only few works transversally research between different approaches and models [8,9]. Due to the existence of a spectrum of metamodels and approaches, it is also challenging for a reliability engineer to select *a priori*, frequently without knowledge about the limit-state function form, the most adequate metamodel for the reliability calculations of a certain problem (in particular if the performance function is implicit). Simpler metamodels (*e.g.* quadratic polynomial) are expected to perform adequately for low complexity limit-state functions, while more complex metamodels (e.g. Kriging) are expected to perform better for highly complex functions. It is not uncommon for the metamodel capability to tackle complex functions to come attached with added effort in the analysis from the understanding and implementation perspectives. It is then of interest to establish some measure of compatibility or hierarchy in metamodeling which may work as a black-box evaluator of an adequate metamodeling approach.

In the present paper, the demand to establish a comparative notional improvement in regard to the type of metamodel used is researched. An innovative approach is proposed in order to tackle problems of reliability analysis that draws its roots from the complement system in immunology [10]. The parallel idea is that of having active

* Corresponding author.
E-mail address: rui.teixeira@ucd.ie (R. Teixeira).

https://doi.org/10.1016/j.ress.2020.107248
Received 21 May 2020; Received in revised form 24 August 2020; Accepted 21 September 2020
Available online 24 September 2020

and inactive models (equivalent to immune defence actors) that tackle the performance function (parallel to invasor) depending on their activation status. Activation and deactivation is triggered by a measure of compatibility with the performance function.

The challenge of active learning using different metamodels is tackled by the introduction of learning and convergence considerations that are metamodel-independent. [11] has previously addressed the demand for universal techniques of learning by introducing three metamodel-independent learning functions. In the context of compatibility, ensembles of metamodels have been developed for multi-metamodel reliability analysis [9]. [12] elaborates on this idea in the selection of metamodels, by studying hierarchy through the influence of the Kriging parameters and assumptions in the metamodeling of a wind turbine. The present research is in-line with the ideas and concerns raised in these works.

It was highlighted that recent trends of adaptive metamodeling in reliability analysis are characterized by an increasing number of techniques and approaches. Five main types of metamodels can be distinguished in the context of reliability analysis: response surfaces (*e.g.*, linear regression with polynomial or radial basis functions) [13,14], Polynomial Chaos Expansions (PCE)[15–17], Support Vector Machines [18,19], Artificial Neural Networks [20], and Kriging models [21,22]. In adaptive metamodeling for reliability, many different methodologies that use these different metamodels emerged in recent years. [13,23] propose multi-stage adaptive implementations with response surfaces that use a quadratic polynomial basis function and nested Latin Hypercube Sampling (LHS). [14] proposed an adaptive response surface that uses radial basis functions and an iterative optimization to enrich the experimental design. [15] proposes the usage of sparsity in metamodeling for reliability, applying it to PCE. [13] extends then the concept of sparsity when applying polynomial basis functions. [24] uses an adaptive reduction of the experimental design (ED) dimension. And, [25] researches on metamodeling definition on an alternative random variable space. The spectrum of methodologies for reliability analysis increases even further when addressing the different learning functions and stopping criteria used. A learning function uses a notion of improvement in order to sequentially improve the metamodeling approximation to the performance function. The efficiency of active learning that uses this notion of improvement generated a proliferation of learning functions for reliability analysis, such as, the Expected Feasibility Function (EFF) [26] the U-function [21], the Least improvement function [27], the adapted U with Failed bootstrap duplicates [17], the universal learning function of [11], the cross-validation learning of [28], the failure pursuit sensitivity of [29] or the reliability expected improvement function [30]. At the same time, further layers of complexity have been added to existing applications by the consideration of further complementary in learning through the combination of different techniques that accelerate the reliability analysis, such as importance sampling [22,31,32], usage of new measures of convergence and accuracy [33–35], parallel sampling [36,37], candidate sample sizes and domain [36,38–40], or learning function randomisation [41]. Moreover, the application of further sampling and hybrid techniques in adaptive approaches [43–45], further extends this batch of alternatives. Kriging models have been particularly relevant in the context of developing new techniques given that, as they enclose an intrinsic measure of uncertainty, they are well suited as self-improving functions [42].

This brief discussion allows to rapidly perceive the large variety that exists in adaptive metamodeling implementations in reliability analysis, which makes it challenging for a reliability engineer to grasp the full extent of this field. It was highlighted that only few works explore a transversal approach to metamodeling and address the challenge that relates a metamodel to the problem in-hand. The purpose of the present work is that of addressing this challenge. For this, Section 2 introduces the topic of reliability analysis using metamodeling, and discusses some of the models used for the effect. Section 3 presents the idea of a complement-basis to metamodeling, discussing concepts of active learning such as, activation and deactivation, learning and stopping criterion. Section 4 presents five examples of application of the complement-basis to solve reliability problems, and discusses implementation and results. Finally, the main conclusions of the work developed are drawn in Section 5.

2. Reliability analysis using metamodels

In the general framework for time-invariant reliability analysis of scalar functions, the probability of failure (P_f) is expressed as the probability $P[\cdot]$ of the performance function $g(x)$ taking values smaller or equal than 0. The probability of failure is then calculated as,

$$P_f = P[g(x) \leq 0] = \int_{g(x)\leq 0} f_x(x)dx \tag{1}$$

where $f_x(x)$ is the continuous joint distribution of d input variables, x (d is the dimension of the space of x). $g(x)$ divides x in two domains: the safe-domain, $g(x) > 0$, and the failure domain, $g(x) \leq 0$.

One of the elementary methods to evaluate the cumbersome integral in Equation (1) is to classify $g(x)$ according to this division in,

$$I_f(x) = \begin{cases} 0, & if \quad g(x) > 0 \\ 1, & if \quad g(x) \leq 0 \end{cases} \tag{2}$$

where I_f is a binary performance evaluator of failure that is $I_f(x) = 1$ in failure and $I_f(x) = 0$ in non-failure. A simple statistical estimator of P_f that uses I_f can be obtained with the Monte Carlo Sampling (MCS) technique and evaluating the following ratio,

$$P_f \approx \hat{P}_f = \frac{1}{N_{MCS}} \sum_{i=1}^{N_{MCS}} I_f(x_i) \tag{3}$$

where N_{MCS} is the total number of random x_i, drawn accordingly to f_x, used to assess the classification of I_f. The coefficient of variation (CoV) of this calculation for a sample size of N_{MCS} is,

$$CoV_{\hat{P}_f} = \sqrt{\frac{1-\hat{P}_f}{N_{MCS}\hat{P}_f}} \tag{4}$$

The low values that are expected for P_f, and consequently large N_{MCS} requirement, constitute a challenge in terms of the analysis time and effort needed to set a meaningful I_F sample. In order to alleviate the calculation of this integral metamodeling is one of the commonly applied alternatives. Metamodels ($\mathbb{M}$) as black box-functions that, in reliability, approximate the costly to evaluate $g(x)$ with a predictor model $G(x)$ appear in different forms, with different contexts of application and assumptions. In the present work, three main types of metamodels are discussed in order to research the complement-basis approach; linear regression with polynomial functions, Polynomial Chaos Expansion (PCE), and Kriging.

2.1. Linear regression with polynomial functions

Linear regression with polynomial functions are the simplest of the existing metamodeling approaches. They are defined as a linear combination of p ($p \in \mathbb{N}^+$) basis functions $[f_1, \cdots, f_p]$ that fit an ED and its respective $g(x)$ evaluations, using weight values a.

$$G(x) = \sum_{h=1}^{p} a_h f_h(x) \tag{5}$$

where the $a = [a_1, \cdots, a_p]^T$ is the set of weight factors that will depend on an ED $[X = x_{ED}, Y = g(X)]$, of size m (m points), used to support the definition of $G(x)$. The ED encloses all the information about $g(x)$ that is used to define $G(x)$ and has critical importance for the metamodeling accuracy. In metamodeling X and Y are respectively defined as a sample of m support points in x and their respective evaluations in $g(X)$.

The basis functions of $G(x)$ may appear in different forms. The most common form is the usage of up to q degree simple polynomials of type x_h^0, x_h^1, x_h^2, x_h^q for $h = 1, \cdots, p$, which is the basis of polynomial regression. Definition of a commonly uses fitting techniques such as the least square regression. Despite limited to some extent (*e.g.*, overfitting in higher order basis functions; or minimum ED size dependence on a), Polynomial functions are appealing due to their relative simplicity.

2.2. Polynomial Chaos Expansion

Polynomial Chaos expansions (PCE) are a metamodel that is able to expand finite variance $g(x)$ processes using a combination of multivariate basis functions that are orthogonal with respect to the joint probability density function f_x of input variables x. PCE dependence on the stochastic inputs and mentioned orthogonal relationship allow $g(x)$ to be well represented by a proper set of basis functions, which perform efficiently in the capture of the global stochastic behaviour of the response [8].

Considering that x is characterized by its f_x, the polynomial chaos expansion of $g(x)$ (on a truncated basis) can be simply written as

$$G(x) = \sum_{i=1}^{P} a_i \Phi_i(x) \tag{6}$$

where a_i are a series of deterministic coefficients and $\Phi_i(x)$ is a basis of multivariate orthonormal polynomials. These multivariate basis polynomials are defined as a tensor of the univariate polynomials related to variables $x = [x_1, \cdots, x_d]$. Definition of $a = [a_1, \cdots, a_P]^T$ also uses a sample of ED points fitted with established techniques, such as, least squares regression.

2.3. Kriging

Kriging models, or Gaussian process models, $G(x)$, are a particular case of metamodel that interpolates $g(x)$ considering that $G(x)$ predictions follow a Gaussian process and approximating the true response function $g(x)$ as

$$G(x) = f(a; x) + Z(x) \tag{7}$$

$$f(a; x) = a_1 f_1(x) + \ldots + a_p f_p(x) \tag{8}$$

$$Z(x) = \mathcal{N}(0, C(x)) \tag{9}$$

where $f(a; x)$ is a polynomial regression in its standard form with p ($p \in \mathbb{N}^+$) basis trend functions $f_p(x)$ and p regression coefficients a to be defined; with p being the number of coefficients that defines the approximation intended in the regression. $Z(x)$ is a Gaussian stochastic process with zero mean. This Gaussian stochastic process is defined with basis on a covariance matrix (C) that relates generic x points by using a constant process variance (σ^2) and a correlation function $R(x; \theta)$ (set on an incremental form of type $x - x_i$ in most cases of reliability, but that can take other forms), and using θ hyperparameters (frequently one for each dimension of the space, but that also function of the correlation used). Such as for the previous metamodels, an ED is required to define $G(x)$.

With Kriging as a metamodel, a prediction of the response for a realisation of a random point x in the space is given by an expected value component ($\mu_{G(x)}$) and a standard deviation component ($\sigma_{G(x)}$). In X, $\mu_{G(X)} = Y$ and $\sigma_{G(X)} = 0$.

3. The complement-basis approach to metamodeling

It was highlighted that the idea of a complement-basis in metamodeling has its roots in the concept of complement system in immunology. The complement system uses a series of activators that enable actors in a batch to change from passive to active depending on the specifications of the problem that needs to be tackled (*e.g.*, in immunology the problem can be a intruder molecule, while in reliability the reciprocate of this is $g(x)$).

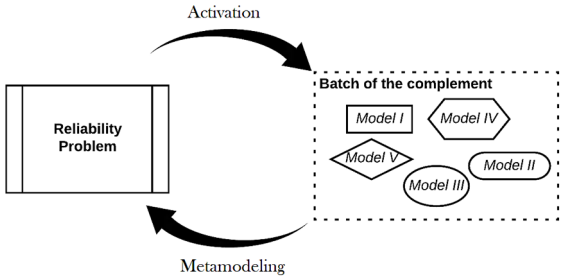

Fig. 1. General description of the complement-basis approach to metamodeling.

Figure 1 presents the conceptualization of the complement-basis approach to metamodeling. When addressing the problem of defining a surrogate of $g(x)$, different models can be applied (each with its assumptions). Reliability engineers are faced with the complex nature of the problem of metamodeling as soon as they are required to choose a model from a batch of existing models and techniques for reliability analysis. The idea of the proposed approach is that of iteratively selecting a metamodel considering its compatibility with the limit-state function. Depending on the function to be addressed, the complement-basis may trigger active model(s) for reliability analysis from a complement-batch, while leaving the remaining models in a dormant state. In some state of the iterative approach metamodels can move from being passive to active and *vice-versa*, accordingly to some activator or activation criteria.

With such implementation it is possible to create a black-box approach without any *prior* assumptions on the limit-state function. Moreover, it can be adapted to be applied in other fields of metamodeling, other than reliability. It is noted also that the degree of complexity that can be used in a complement-basis may depend on the number of activators, passive and active models and their inter-relationship. Such idea can be used to create complement cascades (or chain activation) that may trigger an ensemble of metamodels. It is noted however that [46] identified limited gains when considering more complex metamodel interactions (e.g. weighted ensembles) in detriment of using the most suitable metamodel according to an appropriate surrogate selection criterion. As a result, such implementations that may trigger more complex model interactions may need to be discussed in further detail.

3.1. Multi-metamodel complement-basis

In the present work, in order to illustrate how to construct a complement-basis for reliability analysis, a basis with four metamodels is discussed. A quadratic and cubic polynomial linear regression, a sparse Polynomial Chaos Expansion (PCE) with $P \in [2, 5]$ and a Kriging model with constant trend and Gaussian correlation function are considered to build a complement-basis for active metamodeling. These models are selected in order to be representative of different types of metamodels with different assumptions. The quadratic regression is representative of a simple model, the cubic regression is a slightly more complex model but that is expected to be less stable, the PCE is an even more complex model that uses a more involved basis and that is expected to produce an efficient global approach to smooth functions, and the Kriging (with constant trend and anisotropic Gaussian correlation) is an interpolator that is expected to perform when the limit-state function becomes highly non-linear. The basis as defined may be applied to solve low to moderate dimension reliability problems. Other models can be added to the basis, and its definition may depend on the problem being analysed. One particular instance of relevance in this context is the case of reliability problems that involve a large number of random variables.

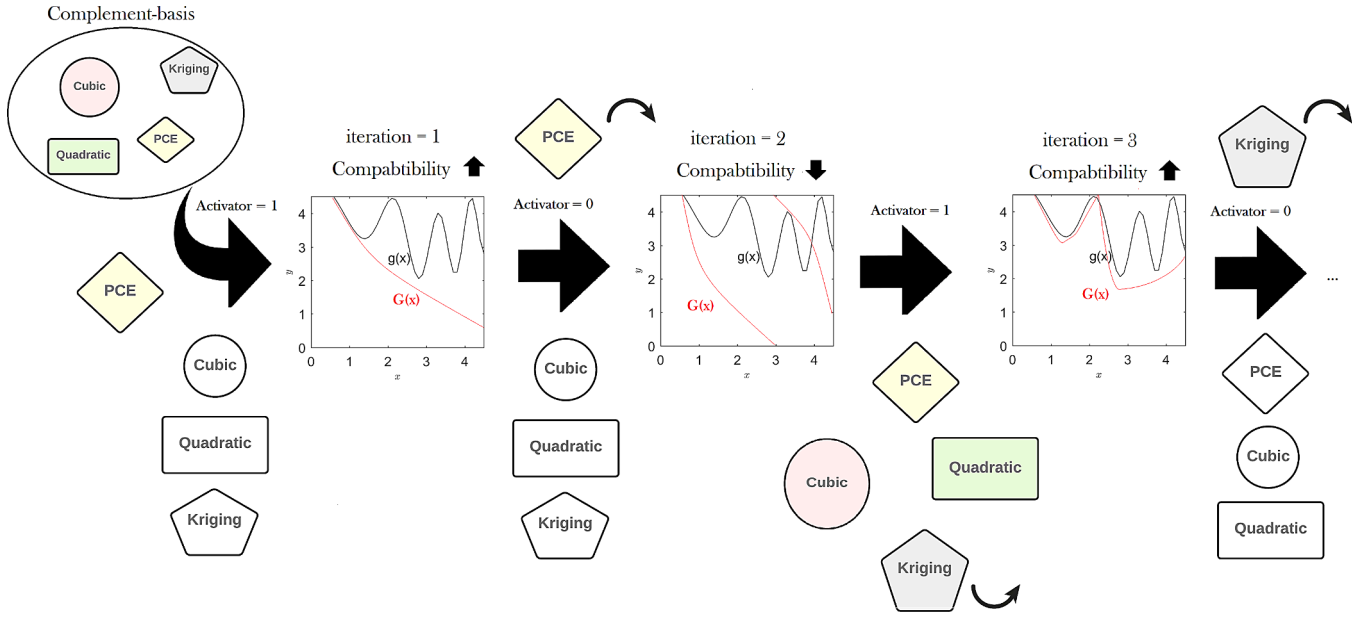

Fig. 2. Illustrative example of complement-basis approach functioning. Note: the figure is only illustrative and is not the result of any implementation procedure.

For high-dimensional problems, which are a highly relevant topic in metamodeling for reliability, it may be of interest to expand the basis to enclose models such as support vector machines. These have synergy with high dimensional problems and were shown to perform with appropriate selection of kernel type and estimation method [47]. An alternative is also to expand the consideration of different parameters for each model of the basis, using a similar rationale to the applied in [12].

An example of a more involved basis can be found in the work of [46], where 24 models are considered to study global surrogate selection. Considering more metamodels in the basis is expected to increase the capability to approximate $g(x)$. However, it is necessary to infer the extent to which more models will increase the prediction accuracy and will not become redundant in relation to the additional effort that is needed to use a larger basis (e.g. calculation of compatibility measures in the present case).

Figure 2 presents an implementation of a complement-basis using the basis selected. The complement-basis has two states, in activation and deactivated. In the beginning of a reliability metamodeling problem the complement structure is in activation. At this point any metamodel can be applied to surrogate $g(x)$. This is illustrated by the colours of the metamodels in Figure 2. A measure of compatibility is then required in order to set the active model. This measure is evaluated for the whole basis and activates the most suitable metamodel. In the illustrative example, it is possible to see that at iteration $(i) = 1$, the PCE becomes the active model while the remaining models become passive (blank state). While the active metamodel improves at new iterations according to some notion of improvement, the activator is disabled. This occurs for the PCE in the passage from $i = 1$ to $i = 2$. If such does not occur (after learning of $i = 2$), the activator is enabled and the measure of compatibility is used to reassess if an alternative metamodel is now more compatible with the function being analysed. Accordingly to this, it is possible to infer that in iteration 3 the Kriging is activated, and the PCE deactivated, as a result of the re-assessment of compatibility for the complement-basis. The Kriging is then enriched, and its compatibility reassessed, as it increases the Kriging stays active in the following iteration.

Some questions emerge when setting the approach described. In particular, two implementation aspects need to be discussed: the measure of compatibility (that will evaluate the adequacy of the metamodels in the basis to surrogate $g(x)$), and the active learning approach (the adaptive implementation applied to the basis selected and the halting evaluator that will guarantee an accurate surrogate). In the present implementation, metamodel-independent measures of activation and learning are considered.

3.2. Measure of compatibility

The average Leave-one-out (LOO) loss is applied as a measure of compatibility in order to select the active metamodel in the adaptive implementation. The interest of the LOO is that it does not demand additional $g(x)$ computations and it can be built using exclusively the i-th ED.

The LOO is a cross-validation technique that consists in measuring the loss $\mathcal{L}$ of a rebuilt metamodel $\mathbb{M}^{X^{k^*}\subset X}$ for each of the m ED points. In each re-definition a subset of the X (X^{k^*}) that excludes the X^k with $k = 1, \cdots, m$ is used to re-build $\mathbb{M}$ as $\mathbb{M}^{X^{k^*}\subset X}$. Then the m $\mathbb{M}^{X^{k^*}\subset X}$ are used to define the respective loss of X^k ($\mathcal{L}_k$) in prediction. The average LOO loss (ϵ_{LOO}) is then given by

$$\epsilon_{LOO} = \frac{1}{m}\sum_{k=1}^{m}\mathcal{L}_k \tag{10}$$

The LOO is almost an unbiased estimator of error [48], and as such is expected to perform as a comparative measure of compatibility of the candidate model from the complement-basis to approximate $g(x)$. [46] showed in a comparative study that this is verified in practice, inferring that the LOO with squared residual loss (here referred to as L2 loss function) is an efficient measure for an adequate selection of global surrogates. [9] applies this same LOO to weight on the adequacy of different metamodels in an ensemble approach. However, in the present example the LOO is applied with absolute deviation loss (here referred to as the L1 loss function), given by

$$\mathcal{L}_k = |g(X^k) - G^{X^{k^*}\subset X}(X^k)| \tag{11}$$

Most adaptive metamodeling techniques for reliability analysis intend to create highly populated ED near the failure region in order to capture the details of it. As a result, in the selection of an active metamodel in an adaptive implementation the error of losing one point in the ED is more likely to be smaller in the failure region where there is more information available about the true function. Hence, if a metamodel has in average a small absolute LOO error then it is expected to be an efficient surrogate of the failure region. Consideration of a

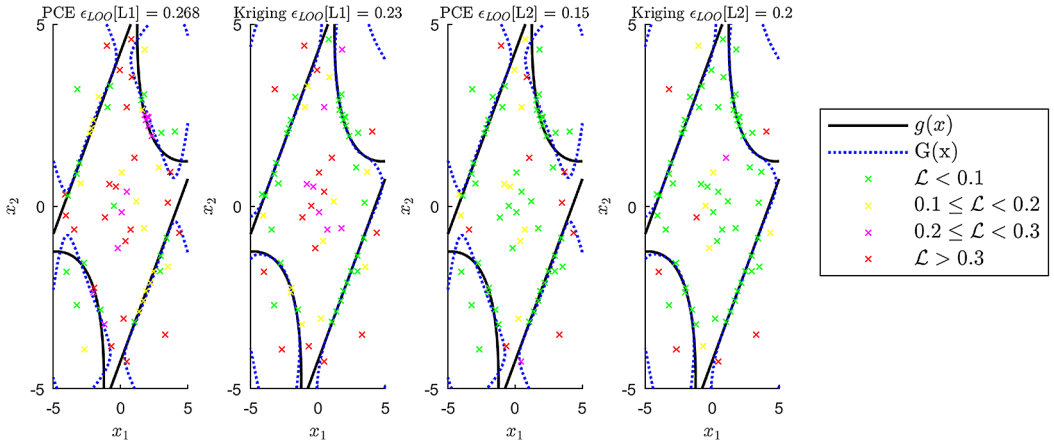

Fig. 3. Comparision of LOO using L1 and L2 loss functions applied to a problem of reliability analysis.

measure of error for selection that minimizes the influence of points with small error (e.g., through the square of the error) and that prioritizes large errors (expected to occur in less populated regions or areas of the x space) may be counter-productive. This is the reason for the choice of the L1 loss function to be preferred for the complement-basis activation in detriment of other widely implemented measures for LOO cross-validation in metamodeling, such as the L2 loss function. The intent is therefore that of capturing the trend of the error in the region of interest.

Figure 3 illustrates the relevance of this consideration. It is possible to see that for two metamodels the L1 loss function prioritizes the Kriging, and that the L2 loss function the PCE. In this case of a relatively complex $g(x)$ with four failure regions, for the presented ED the Kriging approximates better the failure region (Kriging produces an error of less than 1% in P_f prediction, whereas the PCE estimates P_f with an error of 18%). The absolute error in the points near $g(x) = 0$ is mostly green for the Kriging, whereas, for the PCE, even in populated areas, it is recurrently yellow or mangenta. When using the L2 loss these smaller errors are further minimized, and less important ED regions for the problem of reliability start weighting more on the selection of the active metamodel.

To conclude the discussion on the measure of compatibility that sets the activation, simpler models may be activated if the ϵ_{LOO} and the error in the P_f estimation are similar (*e.g.* within an assumption of negligible or comparable deviations) when compared with the more complex models in the basis. It is noted that the LOO already introduces some sense of hierarchy between models.

Quadratic and cubic response surfaces are considered to have lower hierarchy than the Kriging and PCE which are considered to have similar hierarchy (Kriging as a surrogate of local non-linear functions and PCE as a global surrogate of smooth functions). Therefore, if one of the latter is activated, the LOO and P_f estimation of the simpler models should be considered in order to infer if the metamodeling can proceed with a simpler and less expensive to compute model. Section 5 further discusses this consideration in the implementation of the complement-basis to the representative examples.

3.3. Active learning approach

It was highlighted that recent developments in adaptive metamodeling for reliability analysis were characterized by an emergence of multiple learning functions for reliability applications. In the context of using a complement-basis, a measure of learning that is transversal to different types of models is of interest. However, this is not mandatory and different functions can be applied with distinct models (*e.g.*, complement-basis with AKMCS-EFF [26] and bootstrapped PCE [17]).

[11] previously tackled the need for learning approaches that are of transversal application to all metamodeling techniques by proposing three learning functions that depend on: the Euclidean distance, a construct of variance, and a hybrid of both. The learning approach in the present implementation follows the requirements identified in this work. In order to evaluate convergence fo the surrogate, analysis of the reliability problem distribution function is proposed to evaluate the stopping condition for the enrichment of the ED and accurate estimation of P_f. Convergence is considered to be attained when the tail region or region of interest in the tail of the performance function is converged.

3.3.1. Convergence of the density region of interest for P_f prediction

The problem of reliability is that of characterizing $G(x)$ such that P_f can be accurately estimated. In terms of adaptive metamodeling this problem is solved in different forms; it can be attained solving a problem of accurate classification of $I_f(x)$ [21,49], or pursuing to converge the estimation of P_f [27,34].

The pursuit of establishing a $G(x)$ that accurately approximates the reliability calculations for $g(x)$, can be translated to a search for the $P[G(x) \leq 0] \approx P[g(x) \leq 0]$ prediction. Therefore, the problem of reliability can be rewritten as a problem of finding the probability density function of $G(x)$ ($f_{G(x)}$) such that the previous approximation is true. Using this consideration, an universal measure of convergence for metamodeling is proposed in the present work. It uses knowledge of a region of interest in tail of the probability distribution function in order to infer on the improvement of the complement-basis approach. A metamodel allows the definition of $f_{G(x)}$, where P_f represents the lower tail given by $G(x) \leq 0$. As a result, the problem of reliability can be seen from a similar perspective to the problem of finding extreme occurrences in probability theory.

There are different techniques to approximate and evaluate the tail region of a probability density function [50]. One that enables a systematized approach is truncation of the density function at non-*exceedance* percentiles u of interest [51], mitigating the influence of the main body of the distribution in the approximation of the tail or region of interest.

Being $G_u \subset G(x)$ the truncated $G(x)$ at percentile u_1 and u_2, with $u_2 > u_1$ and $u = u_2 - u_1$, and $f_G(x)$ and f_x respectively the distribution function of $G(x)$ and x random variables, then

$$\int_x f_{G_u}(x)dx = \int_{G_u(x)} f_x(x)dx \tag{12}$$

that is, the truncated distribution function $f_{G_u}(x)$ of $f_G(x)$ conditional on G_u encloses the same probability content as the truncated f_x at the same threshold percentiles, and both are equal to u.

A measure of shift between two probability functions f_x and q_x can be given by δ [52], expressed as follows,

$$\delta = \int |f_x(x) - q_x(x)|dx \tag{13}$$

and translated in metamodeling to the total variational change in probability content (δ_P) in iteration i from $f_{G_{u_{i-1}}}(x)$ to $f_{G_{u_i}}(x)$ as

$$\delta_P = \frac{1}{2}\int |f_{G_u^i}(x) - f_{G_u^{i-1}}(x)|dx \tag{14}$$

where, as in [52], the factor $\frac{1}{2}$ is considered for $\delta_P = 1$ in the case where no overlap exists between densities. δ_P represents the shift that occurs in the truncated region accordingly to u in iteration i, considering the effects of the learning by comparing $f_{G_u^i}$ and $f_{G_u^{i-1}}$, *i.e.* the truncated $f_G(x)$ distribution before $(i-1)$ and after (i) the metamodel is updated.

Based on Equation 12, it is possible to construct a measure of accuracy for the truncated u by considering a weighting factor that considers the amount of probability that is enclosed under the truncated region,

$$\delta_{P_u} = \frac{1}{2}\int |f_{G_u^i}(x) - f_{G_u^{i-1}}(x)|dx \int_{G_u(x)} f_x(x)dx \tag{15}$$

and a statistical approximation of this measure can be obtained with MCS,

$$\hat{\delta}_{P_u} = \frac{N_u}{2N_{MCS}} \sum_{o=1}^{n} |f_{G_u^i}(x_o) - f_{G_u^{i-1}}(x_o)| \tag{16}$$

with n being the number of discrete points used to approximate the integral of Equation (14), $f_{G_u}(x_o)$ the corresponding value of the mass function, and N_u the size of the subset of N_{MCS} that encloses the same probability of u. $\hat{\delta}_{P_u}$ can be related to P_f using u. For any u, $\hat{\delta}_{P_u}$ evaluates the sensitivity of the metamodel region of interest to additional information enclosed in the ED or learning procedure.

If $G(x)$ is a perfect metamodel of $g(x)$ then the difference in the distribution of $G(x)$ and $g(x)$ is

$$\hat{\delta}_{P_u}[G(x) \rightarrow g(x)] = 0 \tag{17}$$

and this knowledge is used to infer that as the number of i increase, $G(x)$ is expected to be progressively a closer approximation of $g(x)$, and hence, $\hat{\delta}_{P_u}[G(x)_i \rightarrow G(x)_{i-1}]$ is expected to average to 0 in successive i (as new ED points are not expected to change the distribution of $G(x)$).

Figure 4 -(a) illustrates the rationale behind $\hat{\delta}_{P_u}$ using the tail region,

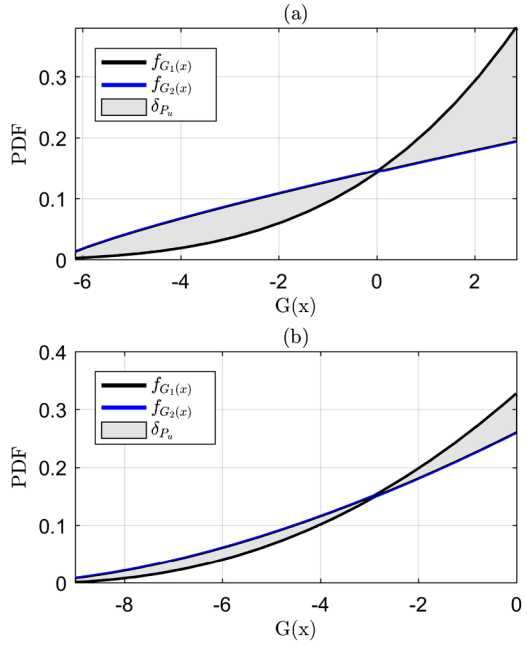

Fig. 4. Examples of truncated density function analysis. PDF - Probability density function.

where both distribution functions enclose the same probability under the curve, u, but different estimates of P_f with $\hat{\delta}_{P_u}$ representing the maximum value relative to u that one estimate may diverge from the other. If the ED is enriched and $\hat{\delta}_{P_u}$ remains unaltered, then it is likely that the new points have not brought relevant information to the problem of estimating P_f.

Analysis of the density function in a region of interest is more informative than inference on P_f, because it also provides information on the rate of change of $G(x)$. Two distinct density functions may generate the same value of P_f however, having large divergence in their tail shape (*e.g.*, one having long tail with very extreme values, while the other has a shorter tail but with large cumulative density, and lower extreme values). The example presented in Figure 4 - (b) depicts such situation. Both truncated distributions enclose the same probability of failure, however, present a difference in the distribution of densities of 17%. Therefore, even considering that both give similar predictions of P_f, the change in $G(x)$ may justify further learning.

It is noted that different values of u to truncate the probability function can be applied, and this may depend on the implementation. In reliability, u must be set to relate to P_f in order to enclose the region of $G(x) = 0$ and to capture more information about: the stability of P_f and how the region of interest and its vicinity are characterized.

If in consecutive i, changes to the failure region prediction are stimulated and $\hat{\delta}_{P_u}$ remains relatively unaltered then the representation of the density region of interest is expected to be robust.

3.3.2. Learning function

In order to set an adaptive ED that stimulates changes in the region of interest, the minimum of the prediction weighted by the Euclidean distance, such as proposed by [11], is used to evaluate new candidates to enrich the ED. [11] results show that limited gains are achieved with more involved metamodel-independent learning functions (estimating measures of uncertainty).

If N_c candidates identified as $x_j = [x_1, \cdots, x_{N_c}]$ are considered, then

$$d_j = \min(d_{X_j}), \qquad j = 1, \cdots, N_c \tag{18}$$

is a measure of distance for the j candidate, where d_X is a vector with the Euclidean distance from the candidate to existing ED points calculated using,

$$d_{Xj} = \left[\sqrt{\sum_{k=1}^{d}(x_j^k - X_1^k)^2}, \sqrt{\sum_{k=1}^{d}(x_j^k - X_2^k)^2}, \cdots, \sqrt{\sum_{k=1}^{d}(x_j^k - X_m^k)^2}\right] \tag{19}$$

and the candidate x_c to be added to the ED is defined as

$$x_c = \arg\min_{x_j}\left(\frac{|G(x_j)|}{d_j^2}\right) \tag{20}$$

This criterion uses local exploitation using the $G(x)$ prediction, and also prioritizes exploration using the Euclidean distance. The addition of the square of the distance enhances exploration of the space (it is noted that it may be removed for large d problems, or replaced by a compatible measure of distance in large d).

Low-discrepancy samples are implemented to generate the set of x_j points. [11] highlighted the interest of having an optimization procedure in the x space in order to find x_c, opting to use MCS due to the large analysis cost that can be expected on the application of the former alternative. In this context of searching x, low-discrepancy samples are an effective technique to set a balanced coverage of the learning space using smaller sample sizes [53]. As x_c depends on the minimum of $G(x)$, when compared with crude MCS, low-discrepancy x_j decreases the selection of x_c that may provide redundant information to the problem of learning (very close in x). In the light of stimulating changes in the density function shape, this feature of low-discrepancy samples is of interest. In the present implementation, low discrepancy samples are

generated using Halton sequences. It is noted that other low discrepancy samples can be used to generate x_j, see [54] for a discussion on different low-discrepancy techniques. Non-relevant candidates in low-discrepancy x_j are truncated with i using a beta-sphere that relates the probability of failure and the remaining probability left outside of the beta-sphere [55,56], $\beta_{HS} = \sqrt{\chi^{-2}(1 - \eta\hat{P}_f^{(i-1)})}$, where β_{HS} is the hypersphere radius that contains the low-discrepancy sample. χ^{-2} is the inverse chi-square distribution function, and η the threshold value of learning space, which is set to be compared with $\hat{P}_f^{(i-1)}$. The set of candidates x_j in iteration i, depends on the present estimation of $\hat{P}_f$, obtained in $i-1$. Assuming that η is set to be small, x_j that are outside of this radius enclose limited information about the problem of reliability and the density region of interest, as a result, are not enclosed in the learning. It is important to remark that this truncation is not a mandatory requirement for a functional implementation, however, as the learning function depends on the Euclidean distance and x_j offers a balanced coverage of x, it mitigates the possibility of learning in regions that have limited interest. The low-discrepancy sample can be also used to estimate P_f, see [30], however, in the present implementation the MCS is used for comparative purposes.

Following the discussion of Section 3.3.1, to halt the adaptive sequence, and conclude the problem of reliability estimation with the complement-basis, $\hat{\delta}_{P_u}$ is used. The learning is halted using $\hat{\delta}_{P_u}$ and a simple moving average (MA) evaluated on the following condition,

$$\frac{1}{\gamma}\sum_{h=i-\gamma+1}^{i}\hat{\delta}_{P_u}^{h} < \epsilon\hat{P}_f^{i} \tag{21}$$

where γ is the i range of the simple MA, and ϵ is an error factor that compares error in the tail region with P_f. In practice this means that changes in the truncated region account in average less than ϵP_f. If $\epsilon = 0.01$, then 1% of the P_f. If in successive i, the leaning function is not able to stimulate changes in the region of interest that account for more than $\epsilon\hat{P}_f$, then the density function of $G(x)$ is expected to provide a robust estimation of the target region.

The stopping criterion presented in [28] is also of interest for a complement-basis implementation. It also uses cross-validation (already used in the proposed approach) and should be investigated in further applications that use similar approaches.

The adaptive metamodeling technique implemented is composed of the following sequential steps, also summarized in Figure 5:

- **Step 1**: Select a batch of metamodels to create the complement-basis. This batch should use *a priori* knowledge on metamodel assumptions to set a complementary basis;
- **Step 2**: Create an initial ED using LHS, a sample of low discrepancy candidates to set x_j, and a MCS sample to estimate P_f. Convert variables to the standard normal space;
- **Step 3**: This step has two states: in activation or deactivated. The algorithm is started in activation. If in activation state, evaluate the complement-basis to select the active model, see Section 3.2. This is achieved using a measure of compatibility, the LOO, complemented by a comparison of model hierarchy. If in deactivated state, progress with the currently active metamodel;
- **Step 4**: Truncate non-relevant x_c accordingly to the present estimation of $\hat{P}_f$;
- **Step 5**: Enrich the ED using the learning approach proposed in the present Section;
- **Step 6**: Update $G(x)$ and evaluate P_f using MCS;
- **Step 7**: Evaluate the divergence in the tail region with $\hat{\delta}_{P_u}$ using $G(x)_i$ (newly enriched model) and $G(x)_{i-1}$(model before enrichment) with the MCS sample. Use the estimation of $\hat{P}_f$ in 6 to define the region of interest. If the region of failure was not yet found use a large value of u (e.g., 0.01) and a detailed characterization of the mass densities.

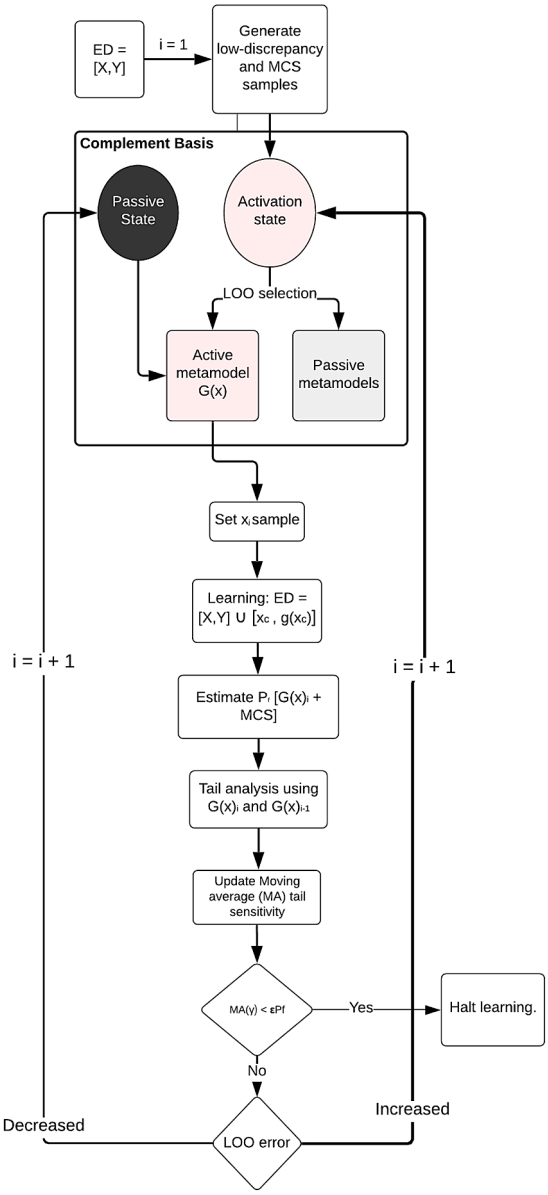

Fig. 5. Complement-basis metamodeling approach scheme.

- **Step 8**: Update the MA. If $i \geq \gamma$, check criterion of Equation 21. If fulfilled, move to step 10, otherwise proceed to 9. If $i < \gamma$, proceed to 9.
- **Step 9**: Update the LOO estimation using the active metamodel and the newly enriched ED. If the LOO increases, return to 3 and activate the complement basis (and calculate the LOO for the remaining models in the batch). If the LOO decreases, return to 3 with the complement basis in deactivated state.
- **Step 10**: Halt the learning, and use the present $G(x)$ as a metamodel of $g(x)$.

A metamodel is activated using the initial ED. This metamodel is then used as a self improving function that selects the new candidate x_c to expand the ED. The ED design is enriched according to the approach introduced. Then the tail sensitivity is calculated in order to infer on the MA. When convergence in the MA is attained the learning is stopped. Otherwise, it progresses with the analysis of the LOO error in order to select if the complement-basis should be activated or not. If it increases it may be indicative of a lower capability of the active model to surrogate the complexity of $g(x)$. Nonetheless, if it is still the most suitable

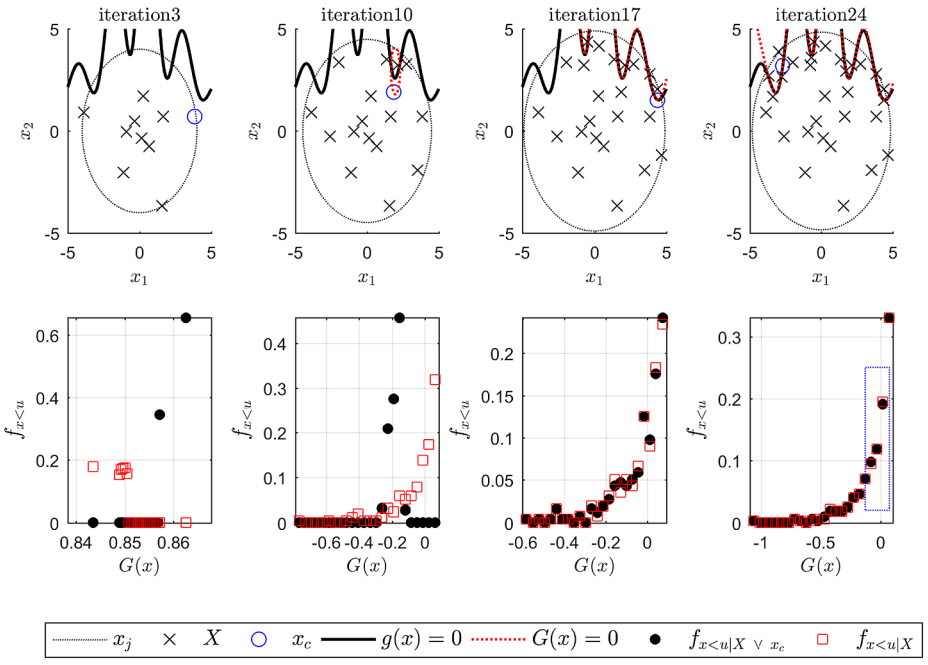

Fig. 6. Example of implementation to two dimensional complex $g(x)$. The threshold u is set to $2P_f$ to compute the lower tails. The ED, $G(x)$ and $g(x)$ representation (top graph) is accompanied by its respective tail description (bottom graph).

model from the basis selected, it will be reactivated again in the activation stage.

Figure 6 presents an example of the learning implementation to a highly complex two-dimensional limit state function. In this case the algorithm is started with a less complex model, but with the progressive increase of knowledge about $g(x)$ the complement-basis activates the Kriging (which is the only model from the batch capable of efficiently approaching this $g(x)$). The idea of the learning function used, and in the absence of efficient alternative to estimate the uncertainty of the basis selected in x for all metamodels, is to stimulate the ED such that the region of interest of the density function of $G(x)$ is stimulated to change. In this example u is set to enclose the lower tail, with cumulative probability equal to twice P_f. It is possible to infer that when the information on $g(x)$ is scarce, the lower tail of $G(x)$ experiences significant changes with the enrichment of the ED. However, as the ED is progressively enriched, new ED points stimulate progressively less the tail region, indicating that it is converging to the true tail. The changes in the lower tail region are an indicator of robustness of the density function estimation in the region of interest. In iteration 24 the density function is close to converge in successive iterations and halt the learning. ED enrichment in this case introduces limited new information in definition of the tail that encloses P_f. All the regions of failure for an accurate estimation of P_f are already identified and the error in the estimation is already under 1%. The lower tail region is stable at this stage.

In applications of reliability analysis, the totality of the lower tail can be used to identify convergence. Nonetheless, there is a region of further interest for accurate P_f estimation; the region highlighted in the (blue) trimmed rectangle of the tail shape in iteration 24. This region encloses a probability equal to P_f in the region of $G(x) = 0$, equally distributed in the safe and failure domains. Hence, if u is defined such that $u = P_f$ and equally distributed around $G(x) = 0$, δ_{P_u} provides an estimate that relates to a change in P_f in the boundary region.

With F_{G^i} as the cumulative distribution function of $G(x)$ in iteration i, and $F_{G^i}^{-1}$ its inverse, this truncated region of $G(x)$, $G_u(x)$ with distribution functions $f_{G_u^i}$ and $F_{G_u^i}$, is defined $\forall i$ by $\left[x_{u_1}^i = F_{G^i}^{-1}\left(\frac{1}{2}u\right), x_{u_2}^i = F_{G^i}^{-1}\left(\frac{3}{2}u\right)\right]$ with,

$$u = \int_{x_{u_1}^i}^{x_{u_2}^i} f_{G^i}(x)dx \tag{22}$$

The change in the truncated u that occurs from $i-1$ to i can be approximated using $F_{G_u^i}$, $f_{G_u^i}$ and $F_{G_u^{i-1}}$, $f_{G_u^{i-1}}$ with

$$\delta_{P_u} = \frac{1}{2}u \int_{\min(x_{u_1}^i, x_{u_1}^{i-1})}^{\max(x_{u_2}^i, x_{u_2}^{i-1})} |f_{G_u^i}(x) - f_{G_u^{i-1}}(x)|dx \tag{23}$$

which again can be estimated with MCS using Equation (16). In the present implementation calculation of $\hat{\delta}_{P_u}$ is approximated using x_0 to characterize the probability mass function with,

$$x_o = \min(x_{u_1}^i, x_{u_1}^{i-1}) + \frac{1}{2}\Delta_o + (o-1)\Delta_o,$$
$$\text{with} \quad \Delta_o = \frac{\max(x_{u_2}^i, x_{u_2}^{i-1}) - \min(x_{u_1}^i, x_{u_1}^{i-1})}{n} \tag{24}$$

and with the mass functions being obtained from the empirical probability distribution with reference to the truncated region and the MCS. If $\hat{\delta}_{P_u} = 1$ then there is no overlapping in densities and the truncated region changed by the value of u from $i-1$ to i, which indicates a total change of position of the region of failure $G(x) = 0$.

The following section discusses examples of implementation. For this purpose, γ is set to 3 and $\epsilon = 0.01$, which means that convergence is attained when changes in the region of interest characterized by $\hat{\delta}_P$ represent in average less than 1% in density the value of $\hat{P}_f$. η in the low discrepancy sequence is 0.05, as there is very low probability of the whole external beta-sphere being misclassified; and $n = 20$ is applied to enable a detailed analysis of the density characterization in the region of interest.

4. Examples of application

Five representative studies of implementation are discussed to illustrate the implementation of the proposed methodology. For these representative examples, the LOO is complemented by inference on model complexity, models are assumed to be comparable when their LOO and $\hat{P}_f$ are close (a maximum of 25% and within a $\pm$ 2.5% range, respectively, is assumed for the representative examples studied), see

Table 1
Average results for the bivariate non-dimensional performance function, Equation (25) and relative comparison with other metamodeling approaches. g_{eval} refers to the average number of $g(x)$ evaluations. The initial ED of the proposed approach uses a LHS of $2d + 3$ points. Low-discrepancy sample uses 10^4 points.

Algorithm	$\hat{P}_f$ ($\times 10^{-5}$)	CoV P_f	e_r(%)	g_{eval}
MCS	2.87	0.03	-	1×10^7
IS* [22]	2.86	0.03	0.0	$19+10^4$
AKMCS-U	2.87	0.03	0.0	23.6
AK-IS* [22]	2.87	0.03	0.0	26.0
iRS* [13]	2.84	-	0.26	16.0
Complement-basis approach[a]	2.87	0.03	0.0	13.0

[a] Active complement: 3^{rd} polynomial function, with minimum value of LOO. Results are based on 10 runs. CoV of g_{eval} of 7.9%.
* Results reported in reference.

Section 3.2. Despite the ultimate goal being the estimation of P_f, LOO considerations are important to complement the reliability prediction, as they are a measure of accuracy of $G(x)$ as a surrogate of $g(x)$ (two models may give the same estimation of P_f, and have different forms).

4.1. Example 1: A non-linear performance function

In the first case a highly non-linear performance function is studied. The performance function for this example is given by $g(x)$

$$g(x) = 0.5 - (x_1 - 2)^2 - 1.5(x_2 - 5)^3 - 3 \tag{25}$$

where both x_1 and x_2 are standard Gaussian variables. This function is representative of a smooth non-linear function in a small dimensional space, and with only a region of failure. Results of the implementation are presented in Table 1.

This non-linear performance function problem is an interesting example that highlights the relevance of using the adequate models in the problem of metamodeling. Both the cubic polynomial and the PCE provide almost perfect surrogates when there are only few points in the ED, making both preferable for this example. Both have LOO that are close to zero, being minimum for the cubic polynomial regression. Both perform even with non-iterative LHS ED that can be decreased to 10 or less points, see Figure 7, where the comparison of fit given for an ED of 10 points is presented for the PCE, Kriging and 3^{rd} polynomial regression. The Kriging with the U function demands almost twice the number of g_{eval}. The iRS of [13] is also highly efficient in approaching this limit-state function, however, slightly less accurate and demanding a more involved analysis.

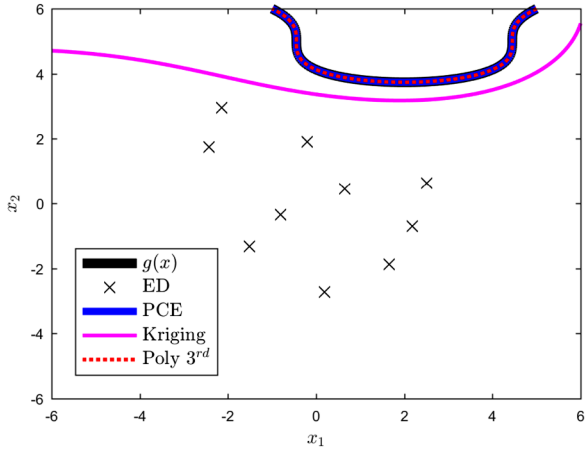

Fig. 7. Example of non-linear limit function prediction using an ED of 10 LHS points for the implemented PCE, Kriging and 3^{rd} degree polynomial regression.

In practical reliability implementations it is not possible to know this (possibility of perfect fit) before-hand as limited knowledge exists about $g(x)$, hence different models need to be tested, such as proposed.

One of the drawbacks of the complement-basis with evaluation of a distribution region of interest and the adaptive approach proposed, and that is illustrated in this example, is that at least γ iterations are demanded to halt the learning. As soon as the cubic polynomial regression is activated, convergence is achieved in γ iterations.

4.2. Example 2: A series system

The series system is one of the most widely studied examples in reliability analysis. This problem is representative of a case where exploration has large importance. There are four distinct regions of failure that need to be accurately characterized to estimate P_f. The limit-state function has global complexity, but is weakly non-linear in each of the branches.

In this example $g(x)$ is defined as,

$$g(x) = \min \begin{cases} g_1(x) = 3 + 0.1(x_1 - x_2)^2 - \frac{x_1 + x_2}{\sqrt{2}} \\ g_2(x) = 3 + 0.1(x_1 - x_2)^2 + \frac{x_1 + x_2}{\sqrt{2}} \\ g_3(x) = (x_1 - x_2) + \frac{6}{\sqrt{2}} \\ g_4(x) = (x_2 - x_1) + \frac{6}{\sqrt{2}} \end{cases} \tag{26}$$

where x_1 and x_2 are random standard Gaussian variables.

Results for the implementation of the complement-basis approach are presented in Table 2.

Results for the proposed approach are comparative to the results presented by some of the most efficient methods used for reliability analysis in this example. The method in average demands about the same number of iterations of some of the most efficient model-based algorithms [9,27,29,39]. In this particular case, the Kriging was the dominant complement, but some iterations use other models in the learning process (occurs when limited information about the performance function exists).

Figure 8 presents implementation results for the complement-basis approach. The algorithm is started with kriging as active and then shifted to the quadratic, cubic and PCE models in iterations 5, 9 and 10 respectively, having the PCE active until iteration 16. In here the complement-basis is altered between Kriging and PCE, which can be identified in this region by the instability of P_f until in iteration 22 the kriging is activated for the remaining of the learning. It is possible to infer that the MA is sensitive to changes in P_f, even when the error in the approximation is already low. Only when the region of failure (u around the density area that separates failure and non-failure) encloses

Table 2
Average results for the bivariate non-dimensional performance function, of Equation (26) and relative comparison with other metamodeling approaches. g_{eval} refers to the average number of $g(x)$ evaluations. Initial ED of the proposed approach uses a LHS of $2d + 3$ points. Low-discrepancy sample uses 10^4 points.

Algorithm	$\hat{P}_f$ ($\times 10^{-3}$)	CoV P_f	e_r(%)	g_{eval}
MCS	4.456	0.02	-	10^6
AKMCS-U	4.455	0.02	0.02	103.8
AKMCS-EFF	4.455	0.02	0.02	114.0
FPS - U* [29]	4.423	-	0.05	64.7
FPS - RD* [29]	4.478	-	0.54	56.5
AKMCS + LIF* [27]	[4.27, 4.54]	-	[0.8, 3.3]	[26, 51]
WAS Ensemble* [9]	4.37	-	1.13	63.0
REAK* [39]	[4.401,4.478]	-	[0.4, 2.1]	[60, 76]
Complement-basis approach[a]	4.437	0.02	0.44	55.2

[a] Active complement: Kriging, with minimum value of LOO. Results are based on 25 runs. CoV of g_{eval} of 18.4%.
* Results reported in reference.

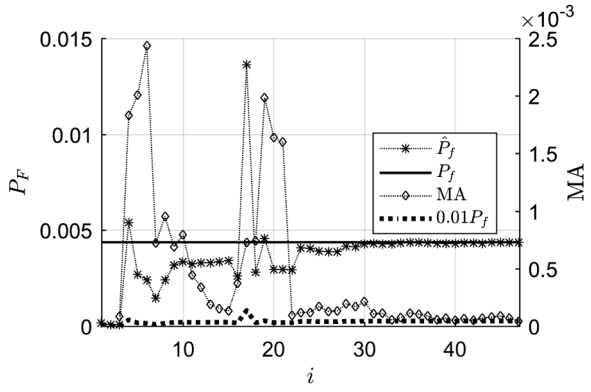

Fig. 8. Example of iteration results for the series system. Black asterisk markers are read on the left vertical axis and diamond markers on the right vertical axis.

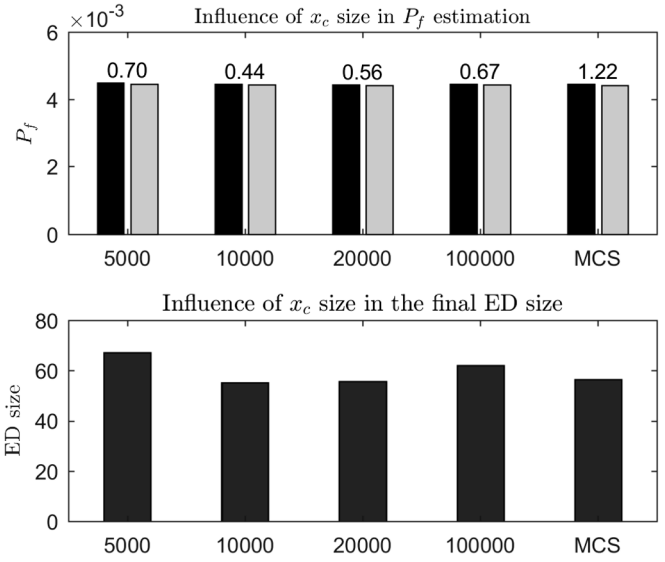

Fig. 9. Influence of the x_j sample in the learning implementation. e_r(%) is presented above the bars of P_f (black bar) and $\hat{P}_f$ (grey bar).

in average a variation in successive iteration of less than 1% of P_f, the algorithm is stopped.

Figure 9 presents average results for the methodology implemented with different low-discrepancy samples of candidates of sizes varying between 5×10^3 and 1×10^5, and with the MCS. The idea of using the low-discrepancy sample is that of fomenting a balanced coverage of x, which allows to decrease the average error in the prediction. It is noted that the MCS is also adequate to apply with the methodology proposed, however attention should be given to the fact that it is occasionally less explorative than the low-discrepancy sample, originating a larger error in the prediction. Additionally, when the ED is small and a simple model is activated this characteristic may lead to a premature halting of the learning.

In LOO error, the Kriging final activation has in average a final LOO that is approximately between 2 to 3 times less than the second model in LOO error (PCE). If the PCE is the only model in the complement, using the same learning procedure, the average number of iterations increases to 66.2, however the error in the approximation increases to 5.7%, which is indicative of the relevance of the choice of the most adequate basis to model the problem. Within the basis of models selected, the Kriging is the only mode capable of providing robust predictions. An example of predictions for the three higher-order models is presented in Figure 10, for the same ED, where it is possible to infer the Kriging capability to outperform the other models in approximating the series system performance function.

4.3. Example 3: Serviceability limit state of non-linear oscillator

The following example concerns the serviceability analysis of a non-linear oscillator. This problem has a medium-low dimensional level, with 6 random variables, and its limit-state function is smooth in the standard normal space. As sparsity is not used in the polynomial regression and to avoid even larger initial ED, in all the examples the cubic polynomial metamodel is activated in the basis only when the ED achieves the minimum size to estimate a.

A rectangular load F with random duration t is applied to the oscillator, with its performance function being defined by the following equation,

$$G(c_1, c_2, m, r, t, F) = 3r - \left|\frac{2F}{m\omega_0^2}\sin\left(\frac{\omega_0 t}{2}\right)\right|, \quad \text{with} \quad \omega_0^2 = \frac{c_1 + c_2}{m} \tag{27}$$

with the characterization of the problem's random variables being presented in Table 3.

Results for the implementation of the a complement-basis are presented in Table 4.

In the case of the oscillator the PCE was the prominent complement to approximate $g(x)$. Figure 11 shows an example of convergence for this problem, where convergence is attained with 36 iterations. $\hat{\delta}_{P_u}$ decreases to halt the algorithm when P_f becomes stable, and changes in the density region of interest become less prominent in more than γ iterations. The gains of using a complement-basis are quite significant when compared with other common implementations of adaptive metamodeling, being only slightly less efficient than the REAK of [39]. In this context, applying $n = 20$ in a relatively small portion of the density function imposes a highly detailed characterization of the densities in this region. If $n = 10$ is applied, g_{eval} is reduced to 34 with no significant loss of accuracy in the prediction of $\hat{P}_f$ ($e_r(\%) = 0.4$). In the case of the series system, if $n = 10$ is applied, g_{eval} is reduced to 47, but with a slight increase of the prediction error ($e_r(\%) = 2.2$). If $n = 30$ is applied, g_{eval} increases to 56.6 ($e_r(\%) = 0.14$) in the oscillator example, and 70.6 ($e_r(\%) = 0.25$) in the series system example.

The particular application of PCE to approximate this smooth function is relevant for the efficiency attained. If the Kriging is forced to be permanently active in the basis, in average the halting of the learning occurs at 60.2 iterations.

Measuring convergence using the tail region has synergy with the LOO. A model with low LOO error, in addition to its expectation of being an accurate $g(x)$ surrogate, is expected to hold better the distribution function shape in the region of interest when the ED is enriched. It is noted that this feature is also related to the complexity of the model (e.g. in polynomials the order of the basis will also influence the capability of the metamodel to change shape when new ED points are added). In the present example the LOO of the final PCE activation was in average between 2 to 3 times smaller than the Kriging, and more than 10 times smaller than the polynomial regressions.

4.4. Example 4: Cantilever tube

The cantilever tube is an interesting example of a limit-state function in a medium dimensional space, with 11 random variables, but that is expected to have a relatively simple shape. The list of random variables in the present example is listed in Table 5. Results for the implementation are presented in Table 6.

The performance function of the cantilever tube is given by,

$$g(x) = S_y - \sqrt{\sigma_x^2 + 3\tau_{zx}^2}, \quad \text{with} \tag{28}$$

$$\sigma_x = \frac{P + F_1 \sin\theta_1 + F_2 sin\theta_2}{A} + \frac{Mr}{I} \tag{29}$$

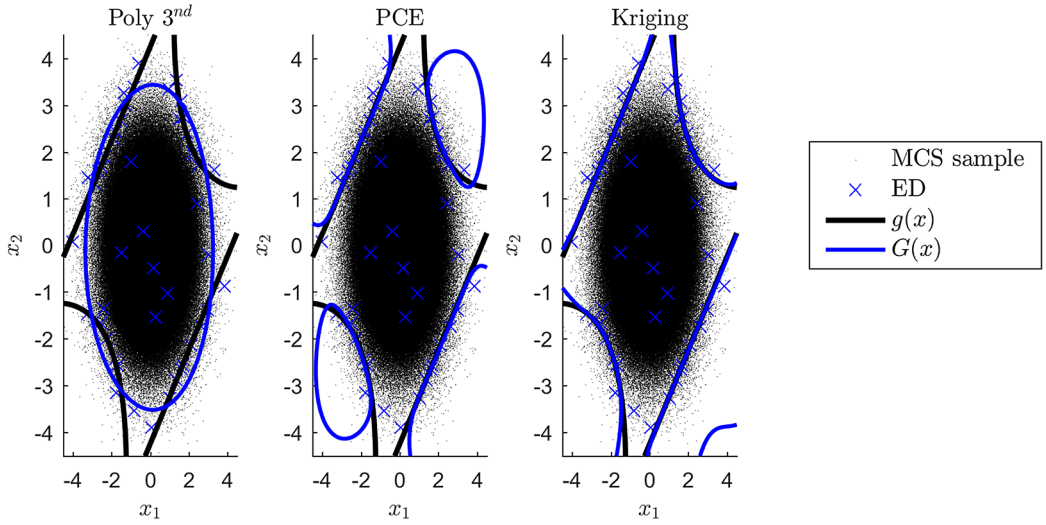

Fig. 10. Example of surrogate approximation given by higher-order models considered in the basis, the 3^{nd} polynomials, PCE and Kriging, for an ED (49 points) obtained with the complement-basis and the proposed active learning implementation.

Table 3
Random variables involved in the problem of serviceability for the non-linear oscillator.

Variable	μ	σ	Distribution
c_1	1	0.1	Gaussian
c_2	0.1	0.01	Gaussian
m	1	0.05	Gaussian
r	0.5	0.05	Gaussian
t	1	0.2	Gaussian
F	1	0.2	Gaussian

Table 4
Average results for the non-linear oscillator and relative comparison with other metamodeling approaches. g_{eval} refers to the number of $g(x)$ evaluations. Initial ED of the proposed approach uses a LHS of $2d + 3$ points. Low-discrepancy sample uses 2×10^4 points.

Algorithm	$\hat{P}_f$ ($\times 10^{-3}$)	CoV P_f	e_r(%)	g_{eval}
MCS	2.851	0.03	-	5×10^4
AKMCS-U	2.86	0.03	0.0	96.4
iRS* [13]	2.82	-	0.55	52.0
AK-ARBIS* [56]	2.831	-	0.1	63.0
REAK* [39]	[2.846,2.864]	-	[0.2,0.6]	[30,40]
Complement-basis approach[a]	2.846	0.03	0.2	43.1

[a] Active complement: PCE, with minimum value of LOO. Results are based on 25 runs. CoV of g_{eval} of 16.7%.
* Results reported in reference.

$$\tau_{xz} = \frac{TD}{2J} \tag{30}$$

$$M = F_1 L_1 \cos\theta_1 + F_2 L_2 \cos\theta_2 \tag{31}$$

$$A = \frac{\pi}{4}[D^2 - (D-2t)^2], \quad I = \frac{\pi}{64}[D^4 - (D-2t)^4], \quad r = \frac{D}{2}, \quad J = 2I \tag{32}$$

In the present case, the gains in the adaptive implementation are achieved with two main models, the 2^{nd} order polynomial response surface and the PCE. When the ED is low the quadratic polynomial is activated due to a lower LOO or due to comparable LOO and P_f estimation. In comparison to AKMCS with U and EFF, the gains of using the quadratic polynomial and the PCE are significant, resulting in approximately half the number of required g_{eval}, with a relatively small trade-off in accuracy (hence the larger CoV obtained in g_{eval}).

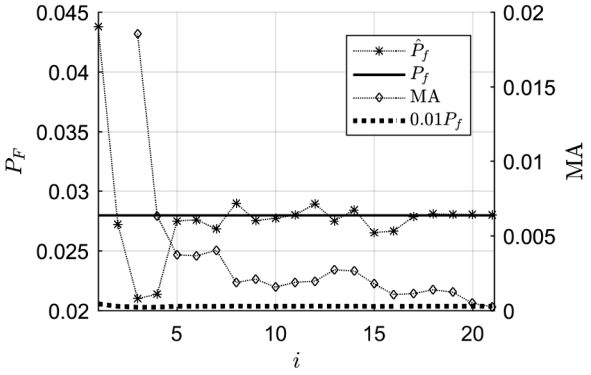

Fig. 11. Example of iteration results for the non-linear oscillator. Black asterisk markers are read on the left vertical axis and diamond markers on the right vertical axis.

Table 5
Random variables of the Cantilever tube problem.

Variable	Parameter 1	Parameter 2	Distribution
$x_1[t(mm)]$	5.0(μ)	0.1(σ)	Gaussian
$x_2[D(mm)]$	42.0(μ)	0.5 (σ)	Gaussian
$x_3[L_1(mm)]$	119.75(*lower bound*)	120.25(*upper bound*)	Uniform
$x_4[L_2(mm)]$	59.75(*lower bound*)	60.25(*upper bound*)	Uniform
$x_5[F_1(kN)]$	3.0(μ)	0.3(σ)	Gaussian
$x_6[F_2(kN)]$	3.0(μ)	0.3(σ)	Gaussian
$x_7[P(kN)]$	12.0(μ)	1.2(σ)	Gaussian
$x_8[T(Nm)]$	90.0(μ)	9.0(σ)	Gumbel
$x_9[S_y(MPa)]$	210.0(μ)	21.0(σ)	Gaussian
$x_{10}[\theta_1(^\circ)]$	5.0(μ)	0.5(σ)	Gaussian
$x_{11}[\theta_2(^\circ)]$	10.0(μ)	1.0(σ)	Gaussian

When the 2^{nd} order polynomial basis model becomes active, and remains as such, convergence is achieved earlier. However, as the ED increases, the PCE tends to overtake the quadratic model, and the algorithm spends additional effort in setting a more accurate $\hat{P}_f$. Figure 12 presents an example of two results for learning implementation where this occurs. The activation of the polynomial metamodel produces efficient results in terms of g_{eval} but with a trade-off in accuracy. It is also possible to infer that the Kriging is the model from the basis that has larger LOO. The trade-off in accuracy of comparable LOO and estimation error was not addressed in detail in the present work, and this selection used only simple assumptions to complement

Table 6
Average results for the bivariate non-dimensional performance function and relative comparison with other metamodeling approaches. g_{eval} refers to the number of $g(x)$ evaluations. Low-discrepancy sample uses 4×10^4 points. Initial ED of the proposed approach uses a LHS of size $2d + 3$. AKMCS uses initial ED of size 10 points.

Algorithm	$\hat{P}_f$ ($\times 10^{-4}$)	CoV P_f	e_r(%)	g_{eval}
MCS	4.304	0.04	-	1×10^6
AKMCS-U	4.303	0.04	0.02	164.6
AKMCS-EFF	4.304	0.04	0.0	189.0
Complement-basis approach[a]	4.266	0.04	0.88	83.6

[a] Dominant complement: PCE, with minimum LOO, and 2^{nd} order polynomial, with minimum LOO or comparable LOO and $\hat{P}_f$. Results are based on 25 runs. CoV of g_{eval} of of 27.5%.

the LOO and $\hat{P}_f$. Further research should comprehensively extend the discussion on this aspect of model selection. If the LOO and P_f are recurrently comparative for a large portion of the adaptive learning for the 2^{nd} order polynomial metamodel and other more complex metamodels, such as the PCE, then $g(x)$ should be expected to be relatively simple (*e.g.*, weak non-linearity in $g(x)$ and failure may be confined to a single region of the space). This consideration, and evaluation of trade-off gains in P_f when using the PCE and simpler models, can provide further insights into the possibility of using simpler metamodels (*e.g* in optimization, if gains in g_{eval} are expected, it may be of interest to allow a larger margin of error than in detailed reliability design).

In terms of computational effort and time it is also of interest to use a simpler model when feasible. The computational effort required to work on larger dimensional examples increases for all models, but with more incidence on complex models such as the Kriging or PCE. Comparative results for the time demanded for 30 and 50 iterations in the present example are presented in Table 7 for two implementations of learning. Even considering the need to calculate the LOO, the time needed to perform the 30 iterations and 50 iterations is slightly reduced. It is noted that these times were computed using the ooDACE Kriging [57] and the PCE of [58]. Times may differ depending on the implementation of the metamodeling algorithms.

Table 7
Average time demanded to solve 30 and 50 iterations for the beam problem with the AKMCS and the complement-basis (PCE as complement). Both use an initial ED of 25 LHS points.

Algorithm	t[30*i*] (s)	t[50*i*] (s)
AKMCS-U	449	934
Complement-basis approach[1]	432	922

It is important to emphasize that these times are expected to have limited relevance when compared with the time that may be demanded to run a finite element analysis or a computational fluid dynamics code multiple times.

4.5. Example 5: Serviceability limit state of a traffic network

The final example studied in the present work is a traffic network in a 19 dimensions space ($d = 19$). This traffic network consists of 13 nodes, 38 links, 66 routes, and 34 origin-destination (OD) pairs, see Figure 13 for a graphical description.

In order to solve the traffic assignment problem to define the traffic cost for the presented network, a User Equilibrium (UE) traffic assignment model is applied. The UE can be defined as: for each OD pair, at user equilibrium, the travel time on all used paths is equal, and (also) less than or equal to the travel time that would be experienced by a single vehicle on any unused path.

This definition was transformed by Beckmann et al. [59] into the following mathematical programming problem. Having a connected transport network, with a set of nodes N, and a set of links A. For certain origin-destination (OD) pairs of nodes, $pq \in D$, where D is a subset of

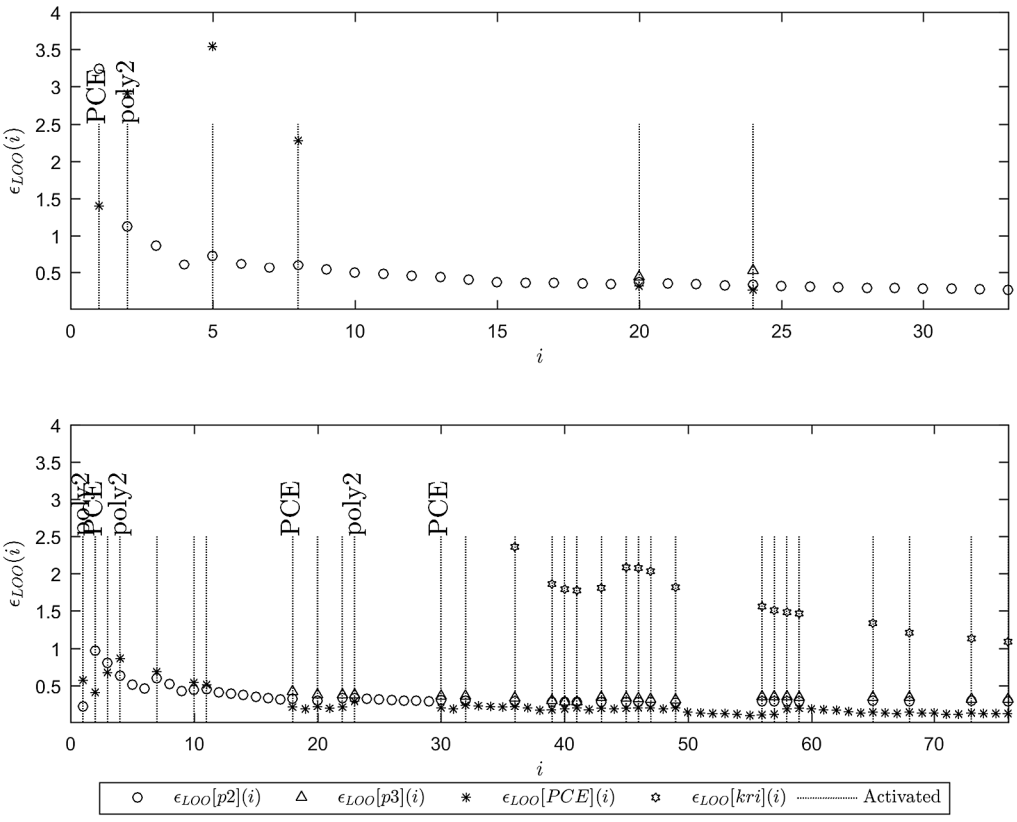

Fig. 12. Convergence results of the learning algorithm for examples: (a) Case where activation converges to the quadratic polynomial (final error in P_f estimation of 1.6%); and (b) Case where activation converges to PCE (final error in P_f estimation of 0.2%). Large LOO ($>$ 4) are not plotted to enhance visualization of the LOO of interest (*e.g.*, Kriging in low *i*). Vertical trimmed lines represent the basis in activation. When the active metamodel is changed, the text above the vertical trimmed line highlights the newly activated model. Initial ED of $2d + 3$ points.

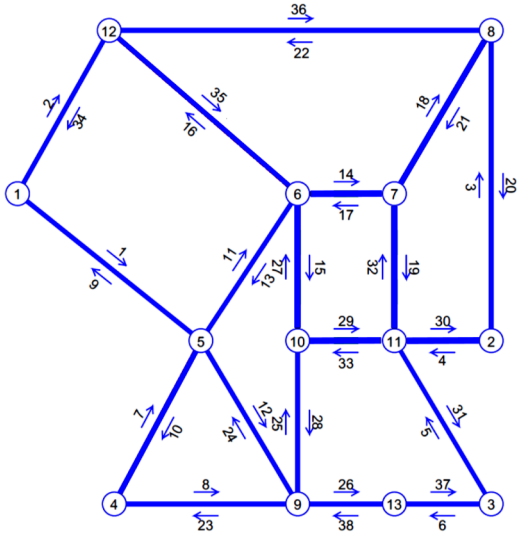

Fig. 13. Nguyen-Dupuis traffic network, graphical description by nodes and links.

NxN, connected by a set of routes R_{pq}, there are given positive demands d_{pq} which give rise to a link flow pattern $\mathbf{v} = (v_a)_{a\in A}$, and a route flow pattern $\mathbf{h} = (h_{pqr})_{r\in R_{pq},pq\in D}$, when distributed through the network.

$$\underset{\mathbf{h},\mathbf{v}}{Minimize} \quad C = \sum_{a\in A} \int_0^{v_a} c_a(s)ds, \tag{33}$$

subject to:

$$\sum_{r\in R_{pq}} h_{pqr} = d_{pq}, \qquad \forall\ (p,\ q) \in D \tag{34}$$

$$\sum_{(p,q)\in D} \sum_{r\in R_{pq}} \delta_{apqr} h_{pqr} = v_a, \qquad \forall\ a \in A \tag{35}$$

$$h_{pqr} \geq 0, \qquad \forall\ r \in R_{pq}\ \forall\ (p,\ q) \in D \tag{36}$$

with

$$\delta_{apqr} = \begin{cases} 1 & \text{if route } r \text{ from node } p \text{ to node } q \text{ contains arc } a; \\ 0 & \text{otherwise,} \end{cases} \tag{37}$$

where ν_a is the link flow, $c_a(\nu_a)$ is the travel cost function for a link a, assuming that it is positive and strictly increasing. A detail description of this methodology and network used can be found in [60,61].

In this example a service failure is assumed to occur when the average travelling time per user of the network increases by t_{C_f} in a day.

19 random variables (x_{OD}), each one representing the statistical distribution of the daily number of users in 19 OD *pq* pairs are considered in the present example. The cost function selected is the well-known Bureau of Public Roads (BPR) function. Failure is analysed using the total traffic cost C for random conditions divided by the number of users in the network (in regard to travelling time), and compared with the standard operational cost (when all the x_{OD} are evaluated in mean values and mean number of users, $C_{\bar{x}_{OD}}$). The performance function of this problem is given by,

$$g(x_{OD}) = 1 + t_{C_f} - \frac{C_{x_{OD}}}{C_{\bar{x}_{OD}}} \tag{38}$$

$C_{\bar{x}_{OD}}$ is the expected cost of travelling in the network for mean values of $\bar{x}_{OD}$, $C_{x_{OD}}$ is the cost of travelling for a random vector of x_{OD}, which is used to compare the value of t_{C_f}. t_{C_f} is equivalent to an average increase of travelling time of t_{C_f} in % per user in a day. Results for the implementation of this example and the capability to surrogate predictions for a MCS sample of 5×10^4 are presented in Table 8.

Knowledge on the network indicates that $g(x)$ should be expected to enclose more than one region of failure, with the performance function varying in a low range of values. Figure 14 presents the learning results for the AKMCS with EFF and U, and the complement-basis. The incremental behaviour of the three learning implementation is illustrative of the mentioned complexity of $g(x)$.

Table 8
Results for the serviceability limit-state function of the network. g_{eval} refers to the number of $g(x)$ evaluations. Low-discrepancy sample uses 2×10^4 points. Initial ED uses a LHS of size $2d + 3$.

$t_{C_f} = 0.15$		
Algorithm	$\hat{P}_f\ (\times 10^{-2})$	g_{eval}
MCS	1.452	5×10^4
AKMCS-U	1.448	637
AKMCS-EFF	1.452	532
Complement-basis approach[1]	1.436	480
$t_{C_f} = 0.20$		
Algorithm	$\hat{P}_f\ (\times 10^{-3})$	g_{eval}
MCS	2.000	5×10^4
AKMCS-U	1.920	415
AKMCS-EFF	2.020	289
Complement-basis approach[a]	1.980	364

[a] Dominant complement: Kriging with minimum LOO.

A reduction of g_{eval} was achieved when comparing with the AKMCS with EFF and U for the case of $t_{C_f} = 0.15$, and with relatively low loss of accuracy. It is noted however that considering convergence of the region of interest with the EFF function allows a reduction of more than 100 iterations (halts the AKMCS-EFF after 378 iterations) with no relevant loss of accuracy (below 1%). In the case of $t_{C_f} = 0.20$, the EFF function showed the best performance. In this case P_f was relatively small in relation to the MCS (only 100 points corresponded to failures). The AKMCS with the U function repeatedly halted the learning prematurely. It is noted with respect to the learning function implemented with the complement that in larger dimensions the Euclidean distance is expected to decrease its efficiency, decreasing the efficiency of the learning in comparison with metamodel-specified functions. Indicators of this characteristic can be identified in the evolution of the accuracy in Figure 14. As d increases, if the complement is given by a complex metamodel, it may of interest to consider adaptation of the basis to use model-specified learning functions such as the EFF.

The gains in computational time are very relevant in both cases, as the initial problem of estimating 5×10^4 samples demanded approximately 100 hours of computational calculations. However, this only occurs for the complement-basis if a full implementation is not pursued, *i.e.* reducing the allocation of analysis time that does not contribute to improve the accuracy of the results (e.g., activating the basis when the ED is already enriched). One particular consideration is that after a certain amount of activations of the complement there is limited interest in testing other than the currently active model. In the present context, the problem of the network is of relevance because it highlights limitations of the complement-basis as defined and objectively indicates new topics of discussion for further implementations. Additional remarks in regard to the present example and that are of large relevance for the efficiency of proposed complement-basis approach and future work are:

- It is of interest to emphasize that a reduced mean LOO activator is expected to perform as well as the full mean LOO. The reduced mean LOO can be evaluated using only the points that are added to the ED or a subset of the ED. This may be of relevance in order to save computational time in future implementations of a complement-basis that uses the LOO as activator. [46] showed before that there is an upper threshold for the number of LOO evaluations that effectively contributes to the accuracy of an efficient estimator of

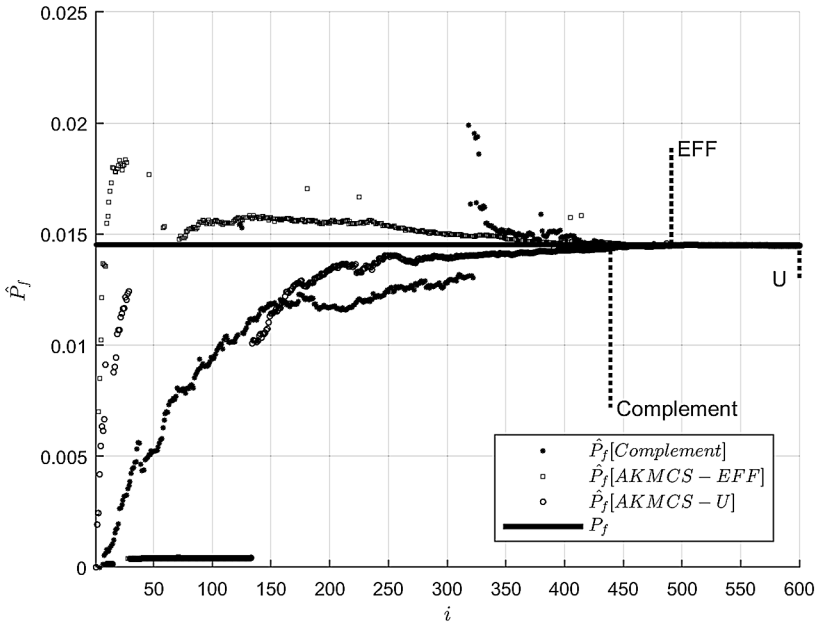

Fig. 14. Results of the adaptive metamodelling for the network function operation with $t_{C_f} = 0.15$.

generalized error with the LOO.

- Above a certain number of iterations there is limited interest in activating the complement-basis (activation tends to the recurrent usage of a single model, see example of Figure 12) which indicates that the learning can proceed without the activation step and keeping the dominant model active when the ED achieves a specified size. This and the previous consideration are of interest to accelerate the implementation in more involved problems such as the presented network example, otherwise, significant computational time is spent without any gain in accuracy. [46] also showed before that in an enriched ED, cross-validation is able to correctly select the best metamodel to approximate different test functions, and in different dimensions.
- With reference to the network example, the need to perform LOO and fit an enriched model justifies the need to reduce the number of activations as the ED increases, in particular because these are not necessary and their cost is significant. In the example of the network if a model is kept active after being repeatedly activated in $t_{cf} = 0.15$ (considering 20 consecutive selections repetition in the basis), the computational time of the analysis is reduced to 11.2 hours. For reference, the AKMCS-EFF solution uses 8.7 hours of implementation (it is important to highlight that in both cases time can be further reduced). A rationale that limits the activation of the basis above a certain threshold is mandatory in the implementation of more involved problems and should be considered in future research.
- Future applications should also infer on the usage of a complementary measure of compatibility, other than the LOO, that may consider explicit information about $g(x)$ (such as a degree of non-linearity).
- Improvements in performance are expected to be achieved with a more detailed analysis of the initial ED. *In tandem* with the lack of a transversal rationales in the application of different metamodels in regard to their adequacy to surrogate a certain $g(x)$ accordingly to model assumptions, the initial ED is rarely addressed as a measure of improvement in the adaptive metamodeling. Recent works, such as [25,62], showed that comprehensively analysing it can contribute to improve the performance of metamodeling.

5. Conclusion

The present work investigates the possibility of using a multiple model implementation using a complement-basis approach in metamodeling for reliability analysis. This work was motivated by the large number of works that emerged in recent years in adaptive metamodeling for reliability analysis, which generated a demand for measures of unification and transversality (between metamodeling approaches) in the field. In the present it is challenging for a reliability engineer to efficiently select a metamodeling approach from the batch of existing techniques without *a priori* information about the problem in-hand, and in particular, the shape of the performance function. Moreover, model assumptions and adequacy to surrogate a certain performance function are rarely addressed in a comprehensive way in the adaptive metamodeling literature. It is of interest to foment interaction between fields of metamodeling. This was identified before to be almost non-existent [8].

The present development builds on ideas from immunology in order to create an approach that iteratively selects suitable metamodels for reliability analysis depending on a measure of expectation or suitability to the problem being addressed. Within different alternative models, one is expected to have more synergy with the problem being analysed. In order to implement a complement-basis, a batch of metamodels is selected and these are set to be in an active or passive state, accordingly to an activator that measures their affinity with the performance function, and also considering their complexity. In this context, selection of the basis should consider different model assumptions and the problem in-hand (e.g. the basis for a reliability analysis of a problem with few random variables will have different requirements than a problem with large number of random variables).

The leave-one-out absolute error is applied as a measure of activation. If a metamodel has relatively low leave-one-out absolute error, it is expected to perform as an efficient boundary of failure for the performance function. Results of the implementation studied confirmed this characteristic.

A learning approach that is metamodel-independent was used in the present research to enable metamodel adaptivity. Convergence was evaluated using information about the sensitivity of the probability density function. This convergence criterion is of particular interest due to its universality in relation to the metamodel used. Nonetheless, the same complement-basis framework can be applied with different

metamodeling approaches, *i.e.* it is not strictly necessary to use the same learning function and stopping criterion for the whole basis. As soon as a metamodel is added to the batch and activated it may use a metamodel-specific learning approach.

It is noted that possible conflicts in redundancy of the learning approach in such case (in case activation shifts the metamodels in the middle of the procedure) need to be checked. As most learning approaches use similar principles of learning, such as searching for the region close to $g(x) = 0$ and(or) using uncertainty measures, it is likely that different learning functions share synergies.

Five examples with different complexities were used to infer on the performance of the proposed method. Results showed that the complement-basis approach can be highly efficient, in particular, exploiting the advantages resulting from the consideration of the (expected) most suitable model to perform a certain reliability analysis. Its performance is at least comparable to some of the most efficient algorithms used for reliability analysis that are constructed for specific metamodels, and it is not uncommon for the gains in efficiency from using an active and adequate selection of different models to be significant. One of the important considerations from the work developed is related to the identification that above a certain number of activations or experimental design size, it is frequent for a single model from the basis to be recurrently selected as active. This indicates that in the complement-basis a level of confidence can be established in relation to whether a model should remain active or the basis activated after a number of activations is performed, a experimental design size is achieved, or a LOO comparative asymptotic behaviour is found. This is an aspect of the implementation that can be used to improve the efficiency of the complement-basis approach. Future works that use a complement rationale should also research on the possibility of using: a reduced leave-one-out error with incidence in regions of interest, comprehensive measures of hierarchy, or new ways of activation that depend on the complexity of the function that is set to be surrogate (e.g., an identifier of non-linearity). Any of three considerations are expected to have large impact in the field of metamodeling for reliability analysis.

CRediT authorship contribution statement

Rui Teixeira: Conceptualization, Methodology, Formal analysis, Investigation, Writing - original draft. **Beatriz Martinez-Pastor:** Methodology, Formal analysis, Validation, Writing - original draft, Writing - review & editing. **Maria Nogal:** Conceptualization, Methodology, Validation, Writing - review & editing. **Alan O'Connor:** Supervision, Funding acquisition, Writing - review & editing.

Declaration of Competing Interest

The authors declare that they have no known competing financial interests or personal relationships that could have appeared to influence the work reported in this paper.

References

[1] Basudhar A, Missoum S. Adaptive explicit decision functions for probabilistic design and optimization using support vector machines. Computers & Structures 2008;86(19-20):1904–17.

[2] Xiao M, Zhang J, Gao L. A system active learning kriging method for system reliability-based design optimization with a multiple response model. Reliability Engineering & System Safety 2020:106935.

[3] Zhang J., Xiao M., Gao L.. A new local update-based method for reliability-based design optimization. Engineering with Computers1–13.

[4] Ribaud M, Blanchet-Scalliet C, Helbert C, Gillot F. Robust optimization: a kriging-based multi-objective optimization approach. Reliability Engineering & System Safety 2020:106913.

[5] Dong Y, Teixeira A, Soares CG. Time-variant fatigue reliability assessment of welded joints based on the phi2 and response surface methods. Reliability Engineering & System Safety 2018;177:120–30.

[6] Wang D, Jiang C, Qiu H, Zhang J, Gao L. Time-dependent reliability analysis through projection outline-based adaptive kriging. Structural and Multidisciplinary Optimization 2020:1–20.

[7] Dong Y, Teixeira A, Soares CG. Application of adaptive surrogate models in time-variant fatigue reliability assessment of welded joints with surface cracks. Reliability Engineering & System Safety 2020;195:106730.

[8] Schobi R, Sudret B, Wiart J. Polynomial-chaos-based kriging. International Journal for Uncertainty Quantification 2015;5(2).

[9] Cheng K, Lu Z. Structural reliability analysis based on ensemble learning of surrogate models. Structural Safety 2020;83:101905.

[10] Carroll M. The complement system in regulation of adaptive immunity. Nature immunology 2004;5(10):981–6.

[11] Xiao N-C, Zuo M, Zhou C. A new adaptive sequential sampling method to construct surrogate models for efficient reliability analysis. Reliability Engineering & System Safety 2018;169:330–8.

[12] Abdallah I, Lataniotis C, Sudret B. Parametric hierarchical kriging for multi-fidelity aero-servo-elastic simulators: Application to extreme loads on wind turbines. Probabilistic Engineering Mechanics 2019;55:67–77.

[13] Guimarães H, Matos JC, Henriques AA. An innovative adaptive sparse response surface method for structural reliability analysis. Structural Safety 2018;73:12–28.

[14] Li X, Gong C, Gu L, Gao W, Jing Z, Su H. A sequential surrogate method for reliability analysis based on radial basis function. Structural Safety 2018;73:42–53.

[15] Blatman G, Sudret B. An adaptive algorithm to build up sparse polynomial chaos expansions for stochastic finite element analysis. Probabilistic Engineering Mechanics 2010;25(2):183–97.

[16] Blatman G, Sudret B. Adaptive sparse polynomial chaos expansion based on least angle regression. Journal of Computational Physics 2011;230(6):2345–67.

[17] Marelli S, Sudret B. An active-learning algorithm that combines sparse polynomial chaos expansions and bootstrap for structural reliability analysis. Structural Safety 2018;75:67–74.

[18] Hurtado JE, Alvarez DA. Classification approach for reliability analysis with stochastic finite-element modeling. Journal of Structural Engineering 2003;129(8):1141–9.

[19] Bourinet JM. Rare-event probability estimation with adaptive support vector regression surrogates. Reliability Engineering & System Safety 2016;150:210–21.

[20] Chojaczyk AA, Teixeira AP, Neves LC, Cardoso JB, Guedes Soares C. Review and application of artificial neural networks models in reliability analysis of steel structures. Structural Safety 2015;52:78–89.

[21] Echard B, Gayton N, Lemaire M. AK-MCS: an active learning reliability method combining kriging and monte carlo simulation. Structural Safety 2011;33(2):145–54.

[22] Echard B, Gayton N, Lemaire M, Relun N. A combined importance sampling and kriging reliability method for small failure probabilities with time-demanding numerical models. Reliability Engineering & System Safety 2013;111:232–40.

[23] Roussouly N, Petitjean F, Salaun M. A new adaptive response surface method for reliability analysis. Probabilistic Engineering Mechanics 2013;32:103–15.

[24] Xu J, Wang D. Structural reliability analysis based on polynomial chaos, voronoi cells and dimension reduction technique. Reliability Engineering & System Safety 2019;185:329–40.

[25] Zhao W, Fan F, Wang W. Non-linear partial least squares response surface method for structural reliability analysis. Reliability Engineering & System Safety 2017;161:69–77.

[26] Bichon B, Eldred M, Swiler L, Mahadevan S, McFarland J. Efficient global reliability analysis for nonlinear implicit performance functions. AIAA journal 2008;46(10):2459–68.

[27] Sun Z, Wang J, Li R, Tong C. LIF: A new kriging based learning function and its application to structural reliability analysis. Reliability Engineering & System Safety 2017;157:152–65.

[28] Xiao N, Zuo M, Guo W. Efficient reliability analysis based on adaptive sequential sampling design and cross-validation. Applied Mathematical Modelling 2018;58:404–20.

[29] Jiang C, Qiu H, Yang Z, Chen L, Gao L, Li P. A general failure-pursuing sampling framework for surrogate-based reliability analysis. Reliability Engineering & System Safety 2019;183:47–59.

[30] Zhang X, Wang L, Sørensen J. REIF: A novel active-learning function towards adaptive kriging surrogate models for structural reliability analysis. Reliability Engineering & System Safety 2019.

[31] Gaspar B, Teixeira A, Guedes Soares C. Adaptive surrogate model with active refinement combining kriging and a trust region method. Reliability Engineering & System Safety 2017;165:277–91.

[32] Zhang J, Xiao M, Gao L, Chu S. A combined projection-outline-based active learning kriging and adaptive importance sampling method for hybrid reliability analysis with small failure probabilities. Computer Methods in Applied Mechanics and Engineering 2019;344:13–33.

[33] Gaspar B, Teixeira A, Guedes Soares C. Assessment of the efficiency of kriging surrogate models for structural reliability analysis. Probabilistic Engineering Mechanics 2014;37:24–34.

[34] Jian W, Zhili S, Qiang Y, Rui L. Two accuracy measures of the kriging model for structural reliability analysis. Reliability Engineering & System Safety 2017;167:494–505.

[35] Wang Z, Shafieezadeh A. On confidence intervals for failure probability estimates in kriging-based reliability analysis. Reliability Engineering & System Safety 2020;196:106758.

[36] Wen Z, Pei H, Liu H, Yue Z. A sequential kriging reliability analysis method with characteristics of adaptive sampling regions and parallelizability. Reliability Engineering & System Safety 2016;153:170–9.

[37] Teixeira R, Nogal M, O'Connor A, Martinez-Pastor B. Reliability assessment with density scanned adaptive kriging. Reliability Engineering & System Safety

2020:106908.
[38] Peijuan Z, Ming W, Zhouhong Z, Liqi W. A new active learning method based on the learning function u of the ak-mcs reliability analysis method. Engineering Structures 2017;148:185–94.
[39] Wang Z, Shafieezadeh A. REAK: Reliability analysis through error rate-based adaptive kriging. Reliability Engineering & System Safety 2019;182:33–45.
[40] Jiang C, Qiu H, Gao L, Wang D, Yang Z, Chen L. EEK-SYS: System reliability analysis through estimation error-guided adaptive kriging approximation of multiple limit state surfaces. Reliability Engineering & System Safety 2020:106906.
[41] Teixeira R, O'Connor A, Nogal M. Adaptive kriging with biased randomisation for reliability analysis of complex limit state functions. 17th International Probabilistic Workshop (IPW2019). 2019.
[42] Teixeira R, Nogal M, O'Connor A, Nichols J, Dumas A. Stress-cycle fatigue design with kriging applied to offshore wind turbines. International Journal of Fatigue 2019;125:454–67.
[43] Bourinet JM, Deheeger F, Lemaire M. Assessing small failure probabilities by combined subset simulation and support vector machines. Structural Safety 2011;33(6):343–53.
[44] Zhang J, Xiao M, Gao L. An active learning reliability method combining kriging constructed with exploration and exploitation of failure region and subset simulation. Reliability Engineering & System Safety 2019.
[45] Xiao S, Oladyshkin S, Nowak W. Reliability analysis with stratified importance sampling based on adaptive kriging. Reliability Engineering & System Safety 2020;197:106852.
[46] Viana FA, Haftka RT, Steffen V. Multiple surrogates: how cross-validation errors can help us to obtain the best predictor. Structural and Multidisciplinary Optimization 2009;39(4):439–57.
[47] Moustapha M, Bourinet J, Guillaume B, Sudret B. Comparative study of kriging and support vector regression for structural engineering applications. ASCE-ASME Journal of Risk and Uncertainty in Engineering Systems, Part A: Civil Engineering 2018;4(2):04018005.
[48] Elisseeff A, Pontil M, et al. Leave-one-out error and stability of learning algorithms with applications. NATO science series sub series iii computer and systems sciences 2003;190:111–30.
[49] Lelièvre N, Beaurepaire P, Mattrand C, Gayton N. AK-MCSi: a kriging-based method to deal with small failure probabilities and time-consuming models. Structural Safety 2018;73:1–11.
[50] Teixeira R, Nogal M, O'Connor A. On the suitability of the generalized pareto to model extreme waves. Journal of Hydraulic Research 2018;56(6):755–70.
[51] Teixeira R., Nogal M., O'Connor A.. Analysis of long-term loading characterization for stress-cycle fatigue design. Wind Energy 22(11):1563–1580.
[52] Borgonovo E. A new uncertainty importance measure. Reliability Engineering & System Safety 2007;92(6):771–84.
[53] Saltelli A, Annoni P, Azzini I, Campolongo F, Ratto M, Tarantola S. Variance based sensitivity analysis of model output. design and estimator for the total sensitivity index. Computer Physics Communications 2010;181(2):259–70.
[54] Kocis L, Whiten W. Computational investigations of low-discrepancy sequences. ACM Transactions on Mathematical Software (TOMS) 1997;23(2):266–94.
[55] Grooteman F. Adaptive radial-based importance sampling method for structural reliability. Structural Safety 2008;30(6):533–42.
[56] Yun W, Lu Z, Jiang X, Zhang L, He P. AK-ARBIS: An improved ak-mcs based on the adaptive radial-based importance sampling for small failure probability. Structural Safety 2020;82:101891.
[57] Couckuyt I, Dhaene T, Demeester P. ooDACE toolbox: a flexible object-oriented kriging implementation. The Journal of Machine Learning Research 2014;15(1):3183–6.
[58] Marelli S, Sudret B. UQLab: A framework for uncertainty in matlab. Proceedings 2nd Int. Conf. on Vulnerability, Risk Analysis and Management (ICVRAM). 2014. p. 2554–63.
[59] Beckmann M, McGuire C, Winsten CB. Studies in the economics of transportation. Tech. Rep.. 1956.
[60] Nogal M, O'Connor A, Caulfield B, Martinez-Pastor B. Resilience of traffic networks: From perturbation to recovery via a dynamic restricted equilibrium model. Reliability Engineering & System Safety 2016;156:84–96.
[61] Martinez-Pastor B. Resilience of traffic networks to extreme weather events: Analysis and assessment. Trinity College Dublin; 2017. Ph.D. thesis.
[62] Fajraoui N, Marelli S, Sudret B. Sequential design of experiment for sparse polynomial chaos expansions. SIAM/ASA Journal on Uncertainty Quantification 2017;5(1):1061–85.